Saturation of conductance in single ion channels: The blocking effect of the near reaction field

Boaz Nadler,[1,*] Zeev Schuss,[2,†] Uwe Hollerbach,[3,‡] and R. S. Eisenberg[3,§]
[1]*Department of Mathematics, Yale University, New Haven, Connecticut 06520, USA*
[2]*Department of Applied Mathematics, Tel-Aviv University, Ramat-Aviv 69978, Israel*
[3]*Department of Molecular Biophysics and Physiology, Rush Medical Center, 1750 Harrison Street, Chicago, Illinois 60612, USA*
(Received 21 June 2004; published 23 November 2004)

The ionic current flowing through a protein channel in the membrane of a biological cell depends on the concentration of the permeant ion, as well as on many other variables. As the concentration increases, the rate of arrival of bath ions to the channel's entrance increases, and typically so does the net current. This concentration dependence is part of traditional diffusion and rate models that predict Michaelis-Menten current-concentration relations for a single ion channel. Such models, however, neglect other effects of bath concentrations on the net current. The net current depends not only on the entrance rate of ions into the channel, but also on forces acting on ions inside the channel. These forces, in turn, depend not only on the applied potential and charge distribution of the channel, but also on the long-range Coulombic interactions with the surrounding bath ions. In this paper, we study the effects of bath concentrations on the average force on an ion in a single ion channel. We show that the force of the reaction field on a discrete ion inside a channel embedded in an uncharged lipid membrane contains a blocking (shielding) term that is proportional to the square root of the ionic bath concentration. We then show that different blocking strengths yield different behavior of the current-concentration and conductance-concentration curves. Our theory shows that at low concentrations, when the blocking force is weak, conductance grows linearly with concentration, as in traditional models, e.g., Michaelis-Menten formulations. As the concentration increases to a range of moderate shielding, conductance grows as the square root of concentration, whereas at high concentrations, with high shielding, conductance may actually decrease with increasing concentrations: the conductance-concentration curve can invert. Therefore, electrostatic interactions between bath ions and the single ion inside the channel can explain the different regimes of conductance-concentration relations observed in experiments.

DOI: 10.1103/PhysRevE.70.051912 PACS number(s): 87.16.Uv, 83.10.Mj, 87.15.Aa

I. INTRODUCTION

Ionic permeation through protein channels embedded in otherwise impermeable cell membranes is one of the most important processes in life [1], governing an enormous range of biological function in health and disease [2]. The ionic current flowing through an open protein channel depends on many factors, reflecting the thermal fluctuations, the concentration gradient, the electrostatic forces, the frictional retarding force on ions in the channel, and the physical forces linking those ions with their environment. These factors in turn depend on the geometry and charge distribution of the channel, the friction within the channel, and obviously, on the bath concentrations on both sides of the channel.

One of the roles of ionic concentration is readily understood. As the surrounding bath concentration is increased, so does the arrival rate of ions to the entrance of the channel, thus increasing the net current. Since ions in the surrounding electrolyte bath diffuse to the channel's mouth, the arrival rate depends linearly on the bath concentrations, at least in a mean-field approximation [4,5].

Standard rate models [1] assume rate constants inside the channel that are independent of bath concentrations and predict a Michaelis-Menten dependence of the current and conductance on the concentration, when the arrival rate of ions from bath to channel is linearly proportional to concentration. *I-C* curves are linear for small bath concentrations, and a saturation of the conductance occurs for high concentrations in these models [1,3].

Some channels indeed exhibit conductance-concentration relations that resemble the Michaelis-Menten law; others, however, exhibit a variety of nonlinear behaviors that deviate from this simple formula. Experiments show that in some channels, conductance depends on the *square root* of the concentration, even at physiological concentrations [6–10], while in other channels conductance (or current) can *decrease* as concentrations increase [11,12]. The latter case, however, typically occurs well beyond physiological concentrations. The inward rectifying K^+ channels [13–15] form an important family of channels for which conductance increases as the square root of concentration. They also show a decrease in conductance as external concentrations are decreased in asymmetrical cases [16–18]. Multisite multi-ion rate models are typically used to explain both the square root dependence of conductance on concentration, in some channels, and the decrease in conductance at high concentrations, in others [14,19], although these models have serious limitations (see, for example, [20,21]).

Such conductance-concentration curves suggest that bath concentrations do more than set the arrival rate of ions to the channel. Indeed, the net current through the channel depends not only on the arrival rate, but also on the force acting on

*Email address: boaz.nadler@yale.edu
†Email address: schuss@post.tau.ac.il
‡Email address: uh@alumni.caltech.edu
§Email address: beisenbe@rush.edu

the ions when they are in the channel pore. These forces, in turn, depend not only on the applied potential and on the channel charge distribution, but also on the bath concentrations, through the long-range Coulombic interactions with the bath ions. We call the component of the force on an ion due to the surrounding bath concentrations the *reaction field force* (RFF).

It seems that the RFF inside the channel has been overlooked in recent literature, in contrast to earlier treatments of [22,23]. Reaction field effects are neglected in traditional rate models, because these models assume (i) hopping rates inside the channel that are independent of concentrations, and (ii) entrance rates into the channel that scale linearly with bath concentrations. The effects of bath concentrations on the forces inside the channel have not been studied by detailed molecular-dynamics (MD) simulations because these simulations typically include only one or two ions inside the pore and few if any ions in the small simulated volume of the surrounding baths [24–27]. Due to their computational complexity, MD simulations are not an adequate tool for the study of these effects, at least in the foreseeable future. A study of these effects by Brownian dynamics simulations, while possibly feasible, would require enormous computer resources, especially in the case of low concentrations, and would likely remain infeasible in the case of nonhomogeneous mixtures that contain trace concentrations, such as a mixture of 100 mM Na-Cl and 10^{-6} M Ca^{2+}. Many, even most biological systems, use trace concentrations of solutes (e.g., cofactors such as Ca^{2+}) as controllers of important biological function [28] and so trace concentrations must be present, and well estimated, if computations are to have biological relevance. Thus, a theoretical study of these effects with continuum models is needed.

Continuum-type models, mainly the Poisson-Nernst-Planck (PNP) system of equations, have been used to describe ionic permeation through protein channels since the early 1990s. However, as was obvious and stated from the beginning, and has become explicit in recent years both in simulations [29–32] and theory [33], standard PNP models provide an inadequate description of currents and concentrations inside narrow pores, because they fail to capture the force components related to the finite size of the mobile ions and to their discrete (rather than continuum) charge distribution.

In previous work [33,34], we showed that the concentration of each ionic species, inside and outside the channel pore, satisfies a Nernst-Planck-type equation, assuming ions are interacting Brownian particles. The average force in the Nernst-Planck equation depends on conditional charge densities and also explicitly includes the dielectric boundary force [35]. Thus, the average force includes the finite size of the ions, and also takes into account the discrete nature of the ion's charge.

The importance of the dielectric boundary force in narrow channels is shown in much recent work [27,29,32,35]. These papers, however, have not studied the effects of the surrounding bath concentrations, e.g., the RFF. In this paper, we consider the effect of bath concentrations on the permeation characteristics of a protein channel that can contain at most one positive ion at a time. Thus, we make a connection to the classical literature of rate theories of single ion channels that is based on detailed electrostatic calculations, including both the dielectric boundary force and the electrostatic effects of the baths.

The study of the permeation characteristics of a single ion channel has a long history. Early approaches were limited to rate models [1], while more modern ones were based on the assumption of diffusive motion of the ion inside the channel [3,36–38]. The main goal of these modeling approaches was to derive a Nernst-Planck equation and boundary conditions that take into account the restriction of the single-ion channel. All of these models, however, assumed that the contribution of the surrounding bath ions is only through the arrival rate to the channel. The electrostatic effects of bath ions were not considered in these models.

In this paper, we study the electrostatic effects of bath ions on the permeating ion inside the channel. We use the implicit solvent ("primitive") model of ionic solutions in which the solvent water molecules are not modeled explicitly, but rather are described electrostatically by an effective dielectric coefficient, and are the source of friction and noise for diffusion. Following Jordan *et al.* [23], we express the single ion channel assumption, by combining a discrete description of the ion inside the channel with a continuum description of the surrounding bath ions. Specifically, we assume that the (conditional) concentrations in the two baths, given the presence of a discrete ion either inside the channel or near its entrance, are described by the solution of the stationary Poisson-Boltzmann equation (in the baths), in the presence of the discrete ion (in or near the channel). The novelty in our approach is the coupling of a discrete ion in the channel with a continuum description of the baths, in order to compute currents with a Nernst-Planck equation.

Our main result is that the force on a discrete ion inside (or near) the channel can be decomposed into almost additive independent terms. These force terms are (i) the interaction force with the fixed charges of the channel (FCF denotes fixed charge force), (ii) the dielectric boundary force (DBF), (iii) the membrane potential force (MPF) due to the applied potential (often assumed to be a constant field), and finally (iv) the reaction field force (RFF) due to the bath concentrations.

By definition, the first three forces are *independent* of bath concentrations. Our calculations show that for a few model channels embedded in neutral lipid membranes, the RFF scales approximately as the *square root* of bath concentrations, a property noticed by [23]. A mathematical explanation for this square root dependence is provided in the Appendix. In addition, we show that the RFF decreases as the radius of the channel increases.

Incorporation of these results into the Nernst-Planck equation shows that different strengths of the reaction field force can lead to different blocking effects and different current-concentration relations. A weak blocking effect and weak reaction field lead to a linear current-concentration relation at low concentrations, as in the Michaelis-Menten formula, while a moderate blocking effect and reaction field lead to a square root dependence of conductance on concentration. A strong blocking and reaction field may even lead to a decrease in the current as concentrations increase. In this

way, our theory explains the observed square root dependence of current on concentration. The square root dependence does not necessarily imply more than one ion inside the channel at any given time nor specific binding sites inside the channel. Of course, other explanations, such as multisite multi-ion rate models, are possible as well.

II. THE REACTION FIELD AND BATH CONCENTRATIONS

We consider the concentration cell used to study transport and membranes in electrochemistry and biophysics. Two electrolyte baths, here with equal concentrations C and relative dielectric coefficient $\varepsilon_b=80$, are separated by an impermeable lipid membrane of dielectric coefficient $\varepsilon_m=2$. Spanning this membrane is a single protein channel that allows ions to go through its pore from one bath to the other. For simplicity, we assume that only positive ions can enter this pore, and that the pore can accommodate at most one ion at a time.

In addition, we consider only the case of a 1-1 simple monovalent electrolyte bathing solution, though our analysis can be easily generalized to more complex electrolytes. Our aim is to compute the ionic current through this channel, given its spatial structure, its permanent charge distribution, the applied voltage, and the surrounding bath concentrations.

Following [33], we start with a Langevin model for the motion of all mobile ions in a finite system, combined with a continuum description of the solvent water molecules. We thus assume that on sufficiently coarse length and time scales, the joint motion of all $2N$ mobile ions can be described by a system of coupled Langevin equations, with independent noise sources,

$$\ddot{\boldsymbol{x}}_j^p + \gamma^p(\boldsymbol{x}_j^p)\dot{\boldsymbol{x}}_j^p = \frac{\boldsymbol{f}_j^p}{m^p} + \sqrt{\frac{2\gamma^p(\boldsymbol{x}_j^p)k_BT}{m^p}}\dot{\boldsymbol{w}}_j^p \ (j=1,2,\ldots,N),$$

$$\ddot{\boldsymbol{x}}_k^n + \gamma^n(\boldsymbol{x}_k^n)\dot{\boldsymbol{x}}_k^n = \frac{\boldsymbol{f}_k^n}{m^n} + \sqrt{\frac{2\gamma^n(\boldsymbol{x}_k^n)k_BT}{m^n}}\dot{\boldsymbol{w}}_k^n \ (k=1,2,\ldots,N), \tag{1}$$

where $\boldsymbol{x}_j^p$ and $\boldsymbol{x}_k^n$ describe the locations of the jth positive and kth negative ions, respectively, while $\boldsymbol{f}_j^p$ and $\boldsymbol{f}_k^n$ are the forces acting on them. In addition, γ^c describes the location-dependent friction coefficient of ions of species c ($c=p,n$), m^c is their effective mass, $\dot{\boldsymbol{w}}_j^p$ and $\dot{\boldsymbol{w}}_k^n$ are Gaussian noises, k_B is Boltzmann's coefficient, and T is the temperature. In this formulation, the water molecules are not represented explicitly. Rather, they are the source of friction and noise, and also determine the effective possibly location-dependent dielectric coefficient. As described in [33,34], we assume that the system is connected to an external control mechanism that maintains a stationary state with constant average concentrations C in the left and right baths, respectively, and a constant average current flowing through the pore, due to a constant applied voltage V between the baths.

In a previous paper [33], we showed that under these assumptions, the steady-state time-averaged concentration of ions of species c, described by $\rho_c(\boldsymbol{x})$, satisfies the Nernst-Planck equation

$$0 = \boldsymbol{\nabla}\cdot\boldsymbol{J}^c(\boldsymbol{x}) = \boldsymbol{\nabla}\cdot\left[\frac{\overline{\boldsymbol{f}}^c(\boldsymbol{x})}{m^c\gamma^c(\boldsymbol{x})}\rho_c(\boldsymbol{x}) - \frac{k_BT}{m^c\gamma^c(\boldsymbol{x})}\boldsymbol{\nabla}\rho_c(\boldsymbol{x})\right], \tag{2}$$

where m^c is the effective mass of the ion, $\gamma^c(\boldsymbol{x})$ is its (location-dependent) friction coefficient, and $\overline{\boldsymbol{f}}^c(\boldsymbol{x})$ is the average force acting on a discrete c-type ion at $\boldsymbol{x}$. This average force is the sum of three terms,

$$\overline{\boldsymbol{f}}^c(\boldsymbol{x}) = \boldsymbol{f}_D^c(\boldsymbol{x}) + \overline{\boldsymbol{f}}_{SR}^c(\boldsymbol{x}) + \overline{\boldsymbol{f}}_{EL}^c(\boldsymbol{x}), \tag{3}$$

where the first term describes the dielectric boundary force [35], the second is the average short-range force, and the third term is the average electrostatic force. The average electrostatic force accounts for all Coulombic interactions of the ion with the other fixed, mobile, and induced charges in the system, excluding the charges induced by the ion itself, which are taken into account by the dielectric boundary force.

The time-averaged electrostatic force on a c ion at $\boldsymbol{x}$ is given by

$$\overline{\boldsymbol{f}}_{EL}^c(\boldsymbol{x}) = -q\boldsymbol{\nabla}\phi_c(\boldsymbol{y}|\boldsymbol{x})\big|_{\boldsymbol{y}=\boldsymbol{x}}, \tag{4}$$

where $\phi_c(\boldsymbol{y}|\boldsymbol{x})$ is the mean (conditional) electrostatic potential at $\boldsymbol{y}$, given an ion of species c at $\boldsymbol{x}$. This potential is the solution of the *conditional* Poisson equation

$$\boldsymbol{\nabla}\cdot[\varepsilon(\boldsymbol{y})\boldsymbol{\nabla}\phi_c(\boldsymbol{y}|\boldsymbol{x})] = -\frac{e}{\varepsilon_0}\left[\rho_{\rm ch}(\boldsymbol{y}) + \sum_j z_j\rho_{j|c}(\boldsymbol{y}|\boldsymbol{x})\right], \tag{5}$$

where $\rho_{\rm ch}(\boldsymbol{y})$ is the fixed charge distribution of the channel and $\rho_{j|c}(\boldsymbol{y}|\boldsymbol{x})$ is the *conditional* density of species j at $\boldsymbol{y}$, given an ion of species c at $\boldsymbol{x}$. For the case of a simple 1-1 monovalent solution and a positive ion at $\boldsymbol{x}$, Eq. (5) becomes

$$\boldsymbol{\nabla}\cdot[\varepsilon(\boldsymbol{y})\boldsymbol{\nabla}\phi_p(\boldsymbol{y}|\boldsymbol{x})] = -\frac{e}{\varepsilon_0}[\rho_{\rm ch}(\boldsymbol{y}) + \rho_{p|p}(\boldsymbol{y}|\boldsymbol{x}) - \rho_{n|p}(\boldsymbol{y}|\boldsymbol{x})],$$

where $\rho_{p|p}$ and $\rho_{n|p}$ are the conditional positive and negative ion concentration profiles, given a positive ion at $\boldsymbol{x}$.

The net current flowing through the channel can be computed from the solution of Eq. (2). Assuming the channel has a narrow, approximately cylindrical pore, whose axis is aligned with the z axis, the net electric current is simply the integral over any cross section in the xy plane of

$$\boldsymbol{J}_z = e(\boldsymbol{J}_z^p - \boldsymbol{J}_z^n),$$

where J_z^c is the z component of the flux vector $\boldsymbol{J}^c$ of species c.

Equation (2), however, cannot be solved unless a specific (closed or computational) form of the conditional densities $\rho_{j|c}(\boldsymbol{y}|\boldsymbol{x})$ is known. As shown in [33], standard PNP theory corresponds to the approximation

$$\rho_{j|c}(\boldsymbol{y}|\boldsymbol{x}) = \rho_j(\boldsymbol{y}).$$

As mentioned in the Introduction, standard PNP neglects both the dielectric boundary force and the short-range forces

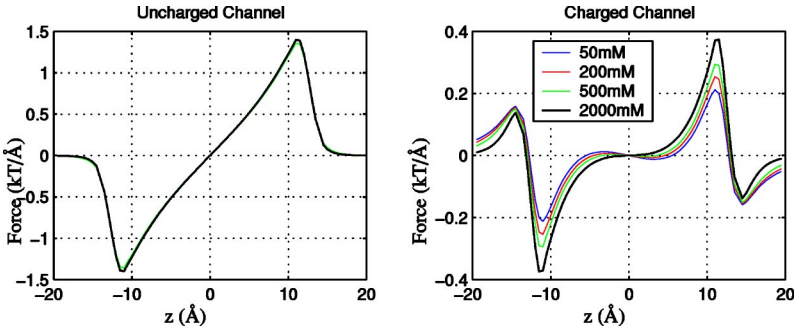

FIG. 1. The electrostatic force on an ion in the uncharged channel (left) and in the charged channel (right).

in Eq. (3). These approximations neglect the finite size of the ions, and more importantly in our case, neglect the fact that, by assumption, the channel can accommodate at most one ion at a time. As shown in theory and in simulations, both of these approximations of standard PNP are oversimplifications that lead to the loss of important properties of narrow channels embedded in low dielectric lipid membranes [33,29–31,27,35].

Here, we adopt a different approximation for these conditional concentrations, which retains the advantage of a continuum description, while taking into account the properties of a single-ion channel assumption. In this paper, we describe the conditional bath concentrations at a continuum level by the steady-state Poisson-Boltzmann equation, in the presence of a discrete ion at $\boldsymbol{x}$. The channel is forced to be singly occupied by no-flux boundary conditions at the two entrances to the channel, on the left and right edges of its pore, imposed when an ion is inside the channel at location $\boldsymbol{x}$. We also include some of the correlation effects of finite size and short-range forces of ions very close to the channel. We impose no flux boundary conditions both at the surface of a sphere of radius 1.5 Å around the center of the ion and at the edges of the channel, just after an ion has exited the pore, thus effectively assuming that no other ion has yet entered the channel. In essence, we have a three-site model, with sites coupled by electrostatics and the one ion assumption.

This approximation retains the notion of a single-ion channel, but neglects both the finite size of ions in the bath away from the channel, and the dielectric boundary force acting on those bath ions. As shown in [35,39], the dielectric boundary force (DBF) on a single ion in the bath is relatively small, because of shielding, and the shielded DBF decreases exponentially with distance from the dielectric wall, rather than the long-range inverse square Coulomb law. We therefore assume that the conditional positive and negative concentrations outside the channel pore, given a positive ion inside the channel at location $\boldsymbol{x}$, follow a Poisson-Boltzmann (PB) distribution,

$$\rho_{p|p}(\boldsymbol{y}|\boldsymbol{x}) = C \exp\left\{-\frac{e\phi(\boldsymbol{y}|\boldsymbol{x})}{kT}\right\},\ \rho_{n|p}(\boldsymbol{y}|\boldsymbol{x}) = C \exp\left\{\frac{e\phi(\boldsymbol{y}|\boldsymbol{x})}{kT}\right\}. \tag{6}$$

The conditional potential $\phi(\boldsymbol{y}|\boldsymbol{x})$—that depends on both the bath ions and the discrete ion inside the channel—is the solution of the Poisson equation,

$$\nabla \cdot [\varepsilon(\boldsymbol{x})\, \nabla\, \phi(\boldsymbol{y}|\boldsymbol{x})] = -\frac{1}{\varepsilon_0}[e\rho_{\mathrm{ch}}(\boldsymbol{x}) + e\rho_{p|p}(\boldsymbol{y}|\boldsymbol{x}) - e\rho_{n|p}(\boldsymbol{y}|\boldsymbol{x}) + q\delta(\boldsymbol{y}-\boldsymbol{x})], \tag{7}$$

where q is the charge of the discrete ion. These approximations lead to electrostatics similar to those computed without concomitant flux [23].

In summary, the presence of a discrete ion (either inside the channel or just outside) leads to a redistribution of the ionic concentrations in the surrounding baths, according to Eqs. (6) and (7). These conditional concentrations, in turn, create a modified force on the discrete ion, according to Eqs. (4) and (5). We call the concentration-dependent component of this force the *reaction field force* (RFF). Thus our formulation accounts for the redistribution of the local bath concentrations near the entrance to the channel, due to the presence of the discrete ion inside it. Note that even when a positive ion is inside the pore, we maintain the assumption that neither a negative nor positive ion can enter the channel: nonelectrical forces, e.g., Lennard-Jones, are assumed to prevent entry of an additional ion into the channel.

III. NUMERICAL RESULTS

We present numerical results, corresponding to the solution of Eqs. (3)–(7) for two different cylindrical channel models. First, we consider an uncharged channel, that is, an ideal cylindrical hole in a dielectric wall, with length $L = 25$ Å and radius $r = 2.5$ Å. Then, we consider a negatively charged channel, with a total charge of $-e$. The fixed charge is spread along a ring ranging from $r = 2.5$ Å to $r = 4.5$ Å and spanning the whole channel. In both of these cases, we numerically solve Eqs. (4)–(7), and present the mean force on a positive ion as a function of its location z on the channel axis.

In Fig. 1, a plot of the force on a monovalent positive ion as a function of location along the channel axis is shown for different bath concentrations, for the uncharged channel (left) and for the charged channel (right). All calculations are given in units proportional to $k_B T$, at room temperature $T = 300$ K. The left graph shows that, for an uncharged channel, there is a strong repulsive force pulling an ion in the channel outwards, towards the bath, from a region of low dielectric coefficient to a region of high dielectric coefficient. In the case of zero bath concentrations, this is the dielectric boundary force (DBF) [35]. The bath concentration also acts on the total force as best seen in Fig. 2, where the difference

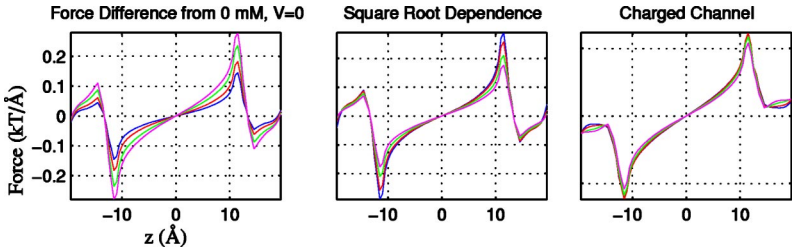

FIG. 2. Left: The difference in electrostatic force from the case of pure water for bath concentrations of 100, 200, 500, and 1000 mM in an uncharged channel. The larger the concentration, the stronger is the reaction field. Middle: same plots, scaled by the square root of concentration. Right: same as middle figure, but for a charged channel.

of the force from the case of zero bath concentration is plotted. The higher the bath concentrations, the larger the total repulsive force driving the ion out of the channel. It is clear from this figure that when the ion is outside the uncharged channel—that is, when $|z|>12.5$ Å—the *effect of the reaction field is reversed*. Then, the force on the charged ion has an opposite sign but the absolute value of the force still increases as concentration increases, essentially shielding the dielectric boundary force near the entrance of the channel.

The corresponding force in a negatively charged channel is shown in the right part of Fig. 1. In comparison to the uncharged channel, the force on a positive ion is now greatly reduced. As in the case of a noncharged channel, the force depends on the bath concentrations, and the higher the bath concentrations, the larger the repulsive force pushing an ion in the channel outwards towards the baths.

We are interested in the study of the reaction field and its dependence on bath concentrations, and so in Fig. 2 (left) we plot the *difference* between the total force at a bath concentration C and the total force with zero bath concentrations. Figure 2 (left) shows these differences for various bath concentrations for the uncharged channel. Similar results (not shown in the graph) occur in the charged channel as well. In the center and rightmost plots of Fig. 2, the same differences are shown for the uncharged and charged channels, respectively (normalized by division by the square root of the difference in bath concentration C). As seen from these graphs, division by the square root of concentration approximately aligns these differences between forces, at concentrations below 1 M.

It seems that as in [23], the electrostatic force $\boldsymbol{F}$ on an ion inside or near the entrance of a narrow channel adopts a simple form, when the applied voltage is zero,

$$\boldsymbol{F}(z,C,V=0) \approx \boldsymbol{F}_{\mathrm{ch}}(z) + \sqrt{C}\boldsymbol{F}_{\mathrm{RF}}(z),$$

where $\boldsymbol{F}_{\mathrm{ch}}(z)$ is the total electrostatic force on an ion at location z, in the case of zero bath concentrations, and $\boldsymbol{F}_{\mathrm{RF}}(z)$ is the unit-normalized reaction field force due to the presence of mobile ions in the surrounding electrolyte baths.

The force $\boldsymbol{F}_{\mathrm{ch}}(z)$ contains the contribution of the dielectric boundary force and of the electrostatic interactions of the mobile ion with the fixed charges of the protein. The reaction field force $\boldsymbol{F}_{\mathrm{RF}}(z)$ contains the contribution of the bath concentrations to the total force. This reaction or blocking force depends on the geometry and fixed charges of the protein and of the lipid membrane, and on the concentration of ions in the bath. A mathematical explanation for the observed square root dependence of the reaction field force on concentration is described in the Appendix, where a simpler problem is analyzed analytically, that of a fixed charge inside an infinite dielectric wall near an electrolyte bath.

The bath concentrations have a stronger effect on an uncharged channel than on a charged channel (Fig. 3). The differences, however, are not large, and both cases yield a potential barrier slightly more than $1\,k_BT$ for a 1 M bath concentration in a channel with radius of 2.5 Å. Also shown in this figure is the corresponding potential barrier for an uncharged channel with radius of 4Å. As expected, the RFF potential is now reduced, in this case by about $0.25\,k_BT$.

An additional potential barrier of $1\,k_BT$ has a significant effect on the single channel conductance because, from Kramer's theory, the escape rate over a potential barrier is proportional to $e^{-\Delta E/k_BT}$. Therefore, even a seemingly small addition of $1\,k_BT$ to the energy difference ΔE leads to a decrease of $1/e \approx 0.37$ in the transition rate over the barrier. Effects of the order of 63% are highly significant when comparing different models of ion permeation. See Sec. IV for further discussion.

Further numerical calculations of the total force, not presented here, show that in the presence of an additional external voltage, the total force on an ion can be approximated,

$$\boldsymbol{F}(\boldsymbol{z},C,V) \approx \boldsymbol{F}_{\mathrm{ch}}(\boldsymbol{z}) + \sqrt{C}\boldsymbol{F}_{\mathrm{RF}}(\boldsymbol{z}) + V\boldsymbol{F}_{\mathrm{ex}}(z), \qquad (8)$$

where $\mathbf{F}_{\mathrm{ex}}(\boldsymbol{z})$ is the force due to the applied external voltage. The formula shows that for small voltages, the effects of bath concentrations are *independent* of the applied voltage, because of the additivity of the force terms $\sqrt{C}\mathbf{F}_{\mathrm{RF}}(\boldsymbol{z})$ and $V\mathbf{F}_{\mathrm{ex}}(\boldsymbol{z})$.

IV. THE REACTION FIELD AND SINGLE CHANNEL CONDUCTANCE

In the previous section, we computed the average force on an ion inside a channel that can accommodate at most one ion at a time, and we showed that the force on the ion is (nearly) the sum of simple components; see the decomposition (8). We now use these results to compute the current flowing through the channel.

For simplicity, we assume that the motion of the mobile ions inside the channel and near its edge is approximately one-dimensional along its axis, with an effective diffusion coefficient D. Because of the close fit of ions in channels, a

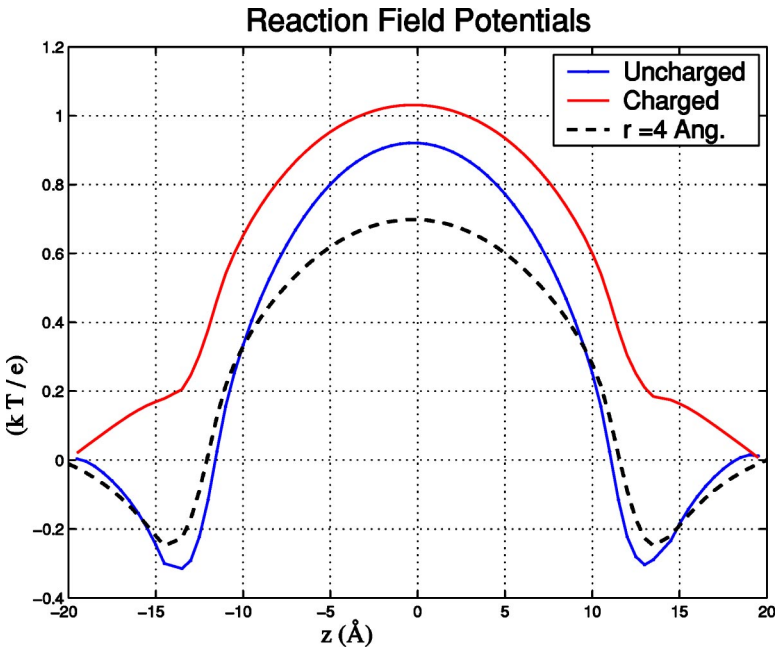

FIG. 3. The reaction field potential ϕ_{RF} corresponding to a bath concentration of 1 M. From top to bottom: charged channel, radius 2.5 Å; uncharged channel, radius 2.5 Å; and uncharged channel, radius 4 Å.

one-dimensional Nernst-Planck equation is likely to be a better model of concentration than a three-dimensional Nernst-Planck equation, with its artifactually large concentrations of ions, e.g., at the membrane-channel boundaries where permanent charges are located. Then, the three-dimensional Nernst-Planck equation (2) for the average concentration inside the channel can be reduced to the simpler one-dimensional version

$$-\frac{d}{dz}J(z)=\frac{d}{dz}D\left[\frac{dc}{dz}+c\frac{e}{kT}\frac{d\phi}{dz}\right]=0.$$

The solution to this equation, for a nondimensional channel of unit length, is given by [3,40]

$$J=D\frac{c(0)e^{e\phi(0)/k_BT}-c(1)e^{e\phi(1)/k_BT}}{\int_0^1 e^{e\phi(z)/k_BT}dz}, \tag{9}$$

where $c(0)$ and $c(1)$ are the concentration values at the edges of the channel. As shown by Levitt [3], for a channel that can accommodate at most one ion at a time and surrounded by symmetric bath concentrations C, the concentrations at the edges of the channel can be approximated by

$$c(0)=c(1)=\frac{C}{1+\gamma C}, \tag{10}$$

where

$$\gamma=LA\int_0^1 e^{-\phi(x)}\left[e^{\phi_{ex}(0)}-\frac{H(x)}{H(1)}(e^{\phi_{ex}(0)}-e^{\phi_{ex}(1)})\right]dx, \tag{11}$$

with ϕ_{ex} the potential corresponding to the external field, L the length of the channel, A its cross-sectional area, and

$$H(x)=\frac{L}{DA}\int_0^x e^{\phi(s)}ds.$$

Assuming the force is given by Eq. (8), the corresponding potential follows a similar decomposition,

$$\phi(z,C,V)=\phi_{ch}(z)+\sqrt{C}\phi_{RF}(z)+V\phi_{ex}(z). \tag{12}$$

Combining Eq. (12) with Eq. (9) gives that for small bath concentrations C,

$$\begin{aligned}\int_0^1 \exp\left\{\frac{e\phi(s)}{k_BT}\right\}ds &= \int_0^1 \exp\left\{e\frac{\phi_{ch}(s)+V\phi_{ex}(s)}{k_BT}\right\}\\ &\quad\times\left(1+\sqrt{C}\frac{e\phi_{RF}(s)}{k_BT}\right)ds\\ &= I_0+\sqrt{C}I_1,\end{aligned} \tag{13}$$

where

$$I_0=\int_0^1 e^{e\phi_{ch}(s)/k_BT}ds,\ I_1=\int_0^1 \frac{e\phi_{RF}(s)}{k_BT}\exp\left(\frac{e\phi_{ch}(s)}{k_BT}\right)ds. \tag{14}$$

For small voltages and small concentrations, the functional relation of current versus concentration takes the form

$$I(C,V)=\text{const}\times V\frac{C}{1+\beta\sqrt{C}}\frac{1}{1+\gamma C}, \tag{15}$$

where $\beta=I_1/I_0$, and γ is given by Eq. (11). This relation is obviously different from the Michaelis-Menten formula,

$$I(C,V)=\text{const}\times V\frac{C}{1+\gamma C}, \tag{16}$$

typically derived for a single ion channel under the assumption that barrier rates inside the channel are independent of bath concentrations. If $\beta\ll 1$ and $\gamma\ll 1$, there is no significant

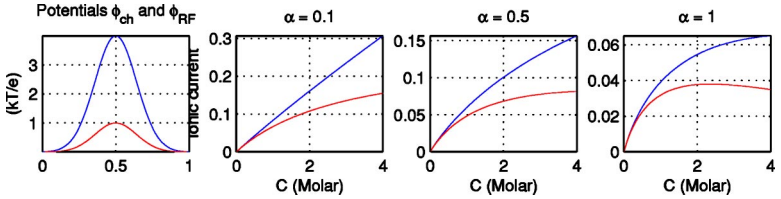

FIG. 4. The potentials ϕ_{ch} and ϕ_{RF} (leftmost graph) and resulting current-concentration relations (in arbitrary units) for three different values of α, the strength parameter of the reaction field (right).

difference between the two formulas for small concentrations. Both predict a linear increase in conductance as a function of concentration. The differences between the two formulas arise when β is not small, as we analyze in the next subsection.

Shielding and possible current-concentration curves

The effects of shielding on the possible current-concentration curves are shown in the following example. We assume that the potential of mean force inside and near the channel has a decomposition like Eq. (12),

$$\phi(z) = \phi_{\mathrm{ch}}(z) + \alpha\sqrt{C}\phi_{\mathrm{RF}}(z) + Vz, \tag{17}$$

where, in this formulation, α measures the strength of the shielding and blocking. Different amounts of shielding correspond to different values of α and give rise to different behaviors of the current as a function of concentration, and thus of the conductance as a function of concentration. For example, the reaction field in a wider channel is smaller than in a narrower channel, thus leading to a smaller value of α.

Specifically, for illustrative purposes we consider analytic expressions for the channel potential and the reaction field potential, of the form

$$\phi_{\mathrm{ch}}(z) = 4\frac{k_BT}{e}\exp\left(-\frac{(z-0.5)^2}{0.1}\right),$$

$$\phi_{\mathrm{RF}}(z) = \frac{k_BT}{e}\exp\left(-\frac{(z-0.5)^2}{0.05}\right), \tag{18}$$

which can correspond to a slightly charged channel, for which the combination of the dielectric boundary force and the interactions with the fixed charges of the channel create a moderate barrier 4 k_BT high, with an additional reaction field barrier of 1 k_BT for a 1 M solution, similar to those computed in Fig. 3. For a specific channel structure, of known or assumed three-dimensional structure and charge distribution, these potentials should be computed from the solution of the relevant Poisson equations.

To compute the current-concentration curve, we insert Eqs. (17) and (18) into the explicit formula (9) with $c(0) = c(1)$ given by Eq. (10) and with a small applied potential of $V = 1\ k_BT/e \approx 25$ mV. For these graphs, we considered a channel of length $L = 25$ Å and cross-sectional area $A = 9\pi$ Å^2. On the left side of Fig. 4, the potentials ϕ_{ch} and ϕ_{RF} are plotted along the nondimensional channel axis z between $z=0$ and $z=1$. The other panels of this figure show I-C curves for three different values of α. The top curves show J with $c(0)=c(1)=C$, while the bottom curves show the predicted flux with the single ion assumption, e.g., with $c(0)$, $c(1)$ given by Eq. (10). For $\alpha=0.1$, as seen from the linear top curve, shielding is negligible, so the current grows linearly with low concentration, and then bends following a Michaelis-Menten formula. For $\alpha=0.5$, shielding is moderate, and the current grows first linearly for small concentrations but then like the square root of the concentration for moderate concentrations. Finally, for $\alpha=1$, shielding is a first-order effect in the force acting on the ion inside the channel. For $\alpha=1$, the current decreases at concentrations around 1 M, because at these concentrations the electrostatic energy required for an ion to leave the electrolyte solution and enter the channel becomes very high. Note that this can also be seen from the theoretical formula (15), since in this case for large concentrations, $I \approx 1/\sqrt{C}$.

In conclusion, our theory explains different conductance-concentration behaviors, based on the effects of the reaction field on an ion either inside or near the channel due to the ions in the surrounding electrolytes.

V. SUMMARY AND DISCUSSION

The permeation of ions through a protein channel is a complex multiscale process, which depends not only on the atomistic details of the protein but also on the configurations of the surrounding baths. Traditional approaches, whether molecular-dynamics simulations or rate models, do not consider the electrostatic effects of the bath ions on the permeation process. Standard continuum formulations, such as the Poisson-Nernst-Planck system of equations, do not adequately describe the dielectric boundary force inside the channel nor the finite size of the ions.

We present a different approach, a hybrid PNP theory that couples a *discrete* description of the contents of the channel with a *continuum* description of the surrounding baths. Our main result is that for a single ion channel embedded in an uncharged lipid membrane, the surrounding bath concentrations create a reaction field whose strength scales with the square root of the bath concentration. The reaction field force (RFF) predicts a square root dependence of conductance on concentration, even with single occupancy. The square root dependence of shielding on concentration should not be surprising, because similar dependences are well known, for example in Onsager's theory of conductance of electrolytes and in the Debye-Hückel theory of ionic shielding [41,42]. We note that when the lipid membrane is charged, the reaction field is quite different in nature and does not typically scale as the square root of the concentration. An analysis of this case will be published elsewhere [43].

Our results are qualitative, and not quantitative, as they must be until we consider a specific protein channel. Moreover, some of our results are limited by the underlying as-

sumptions. For example, our analysis is at the level of the implicit solvent (primitive) model, in which solvent water molecules are described as an effective dielectric coefficient. In addition, we neglect (in the bath) the effects of the finite size of ions. Incorporation of these finite-size effects in homogeneous solutions is a well studied problem, with well established theories such as the mean spherical approximation and the hypernetted chain theory, to name just a few [41,42,44–46]. Appropriate incorporation of similar theories into the confined geometry near and inside a protein channel remains an open research problem [47–51].

APPENDIX A: AN ION INSIDE A DIELECTRIC MEMBRANE

In this section, we investigate the square root dependence of the reaction field force on bath concentrations, using a much simpler setting that allows mathematical analysis.

The three-dimensional space $\mathbb{R}^3$ is composed of two infinite regions, a bath and a membrane, with dielectric coefficients ε_b and ε_m separated by the y-z plane at $x=0$. A single charge q is located at $\boldsymbol{x}_0=(-x_0,0,0)$ inside the membrane, while in the bath region there is a simple 1:1 electrolyte with average concentration ρ at infinity. Note that a similar problem, in which the particle is inside the domain occupied by the electrolyte, rather than inside the dielectric wall, was considered by Stillinger [52].

Let $\phi(\boldsymbol{x}|\boldsymbol{x}_0)$ describe the electric potential throughout space and let $p(\boldsymbol{x}|\boldsymbol{x}_0)$ and $n(\boldsymbol{x}|\boldsymbol{x}_0)$ describe the conditional positive and negative concentrations, given the presence of a discrete positive ion of charge q at $\boldsymbol{x}_0$. Then ϕ satisfies Poisson's equation

$$\boldsymbol{\nabla}\cdot[\varepsilon\,\boldsymbol{\nabla}\,\phi] = -[e(p-n)+q\delta(\boldsymbol{x}-\boldsymbol{x}_0)].$$

We consider an equilibrium mean-field approach, in which the concentrations p and n are the solutions of the Boltzmann equation with the same potential ϕ,

$$p(\boldsymbol{x}) = \rho e^{-e\phi/k_BT},\ n(\boldsymbol{x}) = \rho e^{e\phi/k_BT}.$$

We consider an ion far away from the interface, so the potential ϕ inside the bath is everywhere less than $1k_BT/e$. In this case, linearization of the exponentials leads to the linearized Poisson-Boltzmann equation,

$$\boldsymbol{\nabla}\cdot[\varepsilon\,\boldsymbol{\nabla}\,\phi] = -\left[q\delta(\boldsymbol{x}-\boldsymbol{x}_0) - 2\frac{e^2\rho}{kT}\phi\right].$$

In the two different regions, this equation is

$$\Delta\phi = \begin{cases} \kappa^2\phi, & x>0 \\ -\dfrac{q}{\varepsilon_0\varepsilon_m}\delta(\boldsymbol{x}-\boldsymbol{x}_0), & x<0, \end{cases} \tag{A1}$$

where

$$\kappa = \sqrt{\frac{2e^2\rho}{\varepsilon_0\varepsilon_b k_BT}}$$

is the reciprocal of the Debye length, and equals $\sqrt{\rho}/3.1$ Å for $\varepsilon_b=80$, where ρ is measured in units of molars (moles/liter). We solve Eq. (A1) in cylindrical coordinates, because there is no dependence on the angle θ, but only on the coordinates (x,r). In the region $x<0$, we write $\phi(\boldsymbol{x})=\phi_0(\boldsymbol{x})+\psi(\boldsymbol{x})$, where ψ satisfies a homogeneous Laplace equation, and $\phi_0(\boldsymbol{x})$ is the Coulombic potential created by a point charge q located at $\boldsymbol{x}_0$ in a homogeneous region with uniform dielectric coefficient $\varepsilon(\boldsymbol{x})=\varepsilon_m$. Separation of variables $\psi(\boldsymbol{x})=X(x)R(r)$ gives

$$X'' = \pm\lambda^2 X \text{ and } R'' + \frac{R'}{r} \pm \lambda^2 R = 0. \tag{A2}$$

The corresponding solutions of the modified Bessel equation (A2) with a negative sign are linear combinations of I_0 and K_0, which are singular either at $r=0$ or $r=\infty$. Since ψ is everywhere finite and decays at infinity, all solutions with a negative sign are excluded. In addition, for the positive sign, only one solution of the corresponding Bessel equation, namely, $J_0(r)$, is admissible. The other independent solution, $Y_0(r)$, is singular at $r=0$.

The general solution in this region can then be written as

$$\phi(x,r) = \phi_0(x,r) + \int_0^\infty A(\lambda)J_0(\lambda r)e^{\lambda x}d\lambda, \tag{A3}$$

where $A(\lambda)$ is yet to be determined.

Now consider the homogeneous solution for the region $x>0$. Here separation of variables leads to

$$X'' = \lambda^2 X,\ R'' + \frac{R'}{r} + (\lambda^2-\kappa^2)R = 0. \tag{A4}$$

Similar analysis shows that $\lambda^2 \geqslant \kappa^2$, and therefore the general solution for $x>0$ is

$$\psi(x,r) = \int_0^\infty B(\lambda)J_0(\lambda r)e^{-\sqrt{\lambda^2+\kappa^2}x}d\lambda,$$

where $B(\lambda)$ is another yet undetermined function.

1. Equal dielectric coefficients

First consider the case of equal dielectric coefficients on both sides of the interface, that is, $\varepsilon_b=\varepsilon_m$. In this case, the two constraints on the yet undetermined functions $A(\lambda)$ and $B(\lambda)$ are continuity of the potential and continuity of its normal derivative at $x=0$. These two conditions are

$$\phi_0(0,r) + \int_0^\infty A(\lambda)J_0(\lambda r)d\lambda = \int_0^\infty B(\lambda)J_0(\lambda r)d\lambda,$$

$$\frac{\partial\phi_0(0,r)}{\partial x} + \int_0^\infty \lambda A(\lambda)J_0(\lambda r)d\lambda = -\int_0^\infty \sqrt{\lambda^2+\kappa^2}B(\lambda)J_0(\lambda r)d\lambda.$$

Inserting the expression

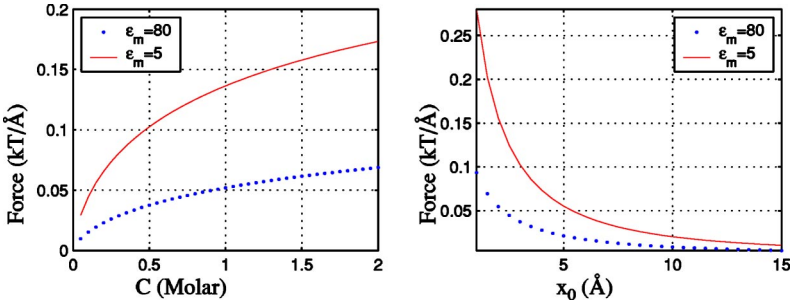

FIG. 5. The electrostatic force on an ion inside a dielectric wall as a function of bath concentration C, at a distance of $x_0=3$ Å from the wall (left), and as a function of the distance x_0, for constant bath concentration of $C=0.5$ M (right).

$$\phi_0(x,r) = \frac{1}{4\pi\varepsilon_m\varepsilon_0}\frac{q}{\sqrt{(x+x_0)^2+r^2}}$$

and rearranging terms gives

$$\int_0^\infty \lambda \frac{A(\lambda)-B(\lambda)}{\lambda} J_0(\lambda r)d\lambda = -\frac{1}{4\pi\varepsilon_m\varepsilon_0}\frac{q}{\sqrt{x_0^2+r^2}},$$

$$\int_0^\infty \lambda\left[A(\lambda)+\frac{\sqrt{\lambda^2+\kappa^2}}{\lambda}B(\lambda)\right]J_0(\lambda r)d\lambda = \frac{1}{4\pi\varepsilon_m\varepsilon_0}\frac{qx_0}{(x_0^2+r^2)^{3/2}}.$$

Using known Hankel transforms, we obtain the linear system of equations

$$A(\lambda)-B(\lambda) = -\frac{q}{4\pi\varepsilon_0\varepsilon_m}e^{-\lambda x_0},$$

$$A(\lambda)+\frac{\sqrt{\lambda^2+\kappa^2}}{\lambda}B(\lambda) = \frac{q}{4\pi\varepsilon_0\varepsilon_m}e^{-\lambda x_0},$$

whose solution is

$$A(\lambda) = \frac{q}{4\pi\varepsilon_0\varepsilon_m}\left[\frac{\lambda-\sqrt{\lambda^2+\kappa^2}}{\lambda+\sqrt{\lambda^2+\kappa^2}}\right]e^{-\lambda x_0}. \quad \text{(A5)}$$

Inserting Eq. (A5) into Eq. (A3), we find that the reaction field force on the discrete charge at $\boldsymbol{x}_0$ is given by

$$\begin{aligned}\boldsymbol{F}(C,\boldsymbol{x}_0) &= -q\frac{\partial}{\partial x}\left[\int_0^\infty A(\lambda)J_0(\lambda r)e^{\lambda x}d\lambda\right]\Bigg|_{(x,r)=(-x_0,0)} \\ &= -\frac{q^2}{4\pi\varepsilon_0\varepsilon_m}\int_0^\infty \lambda\left[\frac{2\lambda}{\lambda+\sqrt{\lambda^2+\kappa^2}}-1\right]e^{-2\lambda x_0}d\lambda.\end{aligned} \quad \text{(A6)}$$

To study the effect of bath concentrations, present inside the coefficient κ, we change variables $\lambda=\kappa\mu$ to obtain

$$\boldsymbol{F}(C,\boldsymbol{x}_0) = \frac{q^2\kappa^2}{4\pi\varepsilon_0\varepsilon_m}\int_0^\infty \mu\frac{\sqrt{1+\mu^2}-\mu}{\sqrt{1+\mu^2}+\mu}e^{-2\kappa x_0\mu}d\mu. \quad \text{(A7)}$$

This is a Laplace transform type integral, for which we have not been able to find a closed-form solution. Asymptotic analysis shows that for large κx_0, the integral is approximately

$$\boldsymbol{F}(C,\boldsymbol{x}_0) = \frac{q^2\kappa^2}{4\pi\varepsilon_0\varepsilon_m}\frac{1}{(2x_0)^2},$$

so that for either very large concentrations or very large distances from the wall, the reaction field increases linearly as a function of concentration. The other extreme—when x_0 is very close to the wall—is inconsistent with the linearization of the nonlinear PB equation.

In our biological application, we are interested in distances which are of the order of a few angstroms, and concentrations that range between 50 mM and 2 M. In this range, $\kappa x_0=O(1)$. Expansion of Eq. (A7) in powers of κx_0-1 gives

$$\begin{aligned}\boldsymbol{F}(C,\boldsymbol{x}_0) = &\frac{q^2}{4\pi\varepsilon_0\varepsilon_b(2x_0)^2} \\ &\times[0.275+0.237(\kappa x_0-1)]+O(\kappa x_0-1)^2,\end{aligned}$$

with similar expansions near other values of κx_0. Because κ scales like the square root of the concentration, we obtain a square root dependence of the force on concentration.

2. Different dielectric coefficients

In the case $\varepsilon_m\neq\varepsilon_b$, the continuity equations are

$$A(\lambda)-B(\lambda) = -\frac{q}{4\pi\varepsilon_0\varepsilon_m}e^{-\lambda x_0},$$

$$\varepsilon_m A(\lambda)+\varepsilon_b\frac{\sqrt{\lambda^2+\kappa^2}}{\lambda}B(\lambda) = \varepsilon_m\frac{q}{4\pi\varepsilon_0\varepsilon_m}e^{-\lambda x_0}.$$

Solving for $A(\lambda)$ gives

$$A(\lambda) = \frac{q}{4\pi\varepsilon_m\varepsilon_0}\frac{\lambda-\varepsilon_r\sqrt{\lambda^2+\kappa^2}}{\lambda+\varepsilon_r\sqrt{\lambda^2+\kappa^2}}e^{-\lambda x_0},$$

where $\varepsilon_r=\varepsilon_b/\varepsilon_m$. Therefore, the force at the fixed charge location is

$$\boldsymbol{F}(C,x_0) = \frac{q^2}{4\pi\varepsilon_m\varepsilon_0}\int_0^\infty \lambda \frac{\lambda^2(\varepsilon_r^2-1)+\varepsilon_r^2\kappa^2}{(\lambda+\varepsilon_r\sqrt{\lambda^2+\kappa^2})^2} e^{-2\lambda x_0} d\lambda.$$

Note that when there are no bath concentrations, $C=0$, that is $\kappa=0$, we obtain that

$$\boldsymbol{F}(0,x_0) = \frac{q^2}{4\pi\varepsilon_m\varepsilon_0}\int_0^\infty \frac{\varepsilon_r-1}{\varepsilon_r+1}\lambda e^{-2\lambda x_0} d\lambda$$

$$= \frac{q^2}{4\pi\varepsilon_m\varepsilon_0}\frac{\varepsilon_r-1}{\varepsilon_r+1}\frac{1}{(2x_0)^2},$$

which is the familiar expression for the dielectric boundary force on a particle near a dielectric wall.

Because we are interested in the effects of the bath concentrations on the overall force, we consider the difference $\delta\boldsymbol{F}(C,x_0)=\boldsymbol{F}(C,x_0)-\boldsymbol{F}(0,x_0)$, which removes the purely dielectric component due only to the different dielectric coefficients of the two regions. We have then

$$\delta\boldsymbol{F}(C,x_0) = \frac{q^2\kappa^2}{4\pi\varepsilon_0\varepsilon_m}\frac{2\varepsilon_r}{\varepsilon_r+1}\int_0^\infty \mu \frac{\sqrt{\mu^2+1}-\mu}{\varepsilon_r\sqrt{\mu^2+1}+\mu} e^{-2\kappa x_0\mu} d\mu,$$

which indeed reduces to Eq. (A6) when $\varepsilon_r=1$. Similar analysis shows that this force also increases as the square root of the concentration when $\kappa x_0=O(1)$.

In Fig. 5, the force as a function of bath concentrations is plotted for a charged particle at a distance of 3 Å from the wall (left) for two cases, one with $\varepsilon_b=\varepsilon_m=80$ and the other with $\varepsilon_m=5$. Note that in the case of a dielectric wall, the force is stronger than in its absence, because the force bath ions exert on the fixed ion is larger in this case. Moreover, the shielding force decreases monotonically as a function of ε_m, for fixed ε_b. Specifically, the shielding force more than doubles when ε_m is reduced from 80 to 5.

[1] B. Hille, *Ionic Channels of Excitable Membranes*, 2nd ed., (Sinauer Associates, Sunderland, MA, 1992).
[2] F.M. Ashcroft, *Ion Channels and Disease* (Academic, New York, 1999).
[3] D.G. Levitt, Annu. Rev. Biophys. Biophys. Chem. **15**, 29 (1986).
[4] J. Bockris and A.K. Reddy, *Modern Electrochemistry*, 2nd ed. (Plenum, New York,1998).
[5] B. Nadler, T. Naeh, and Z. Schuss, SIAM (Soc. Ind. Appl. Math.) J. Appl. Math. **62**, 433 (2001).
[6] E. Cooper and A. Shrier, J. Gen. Physiol. **94**, 881 (1989).
[7] C. Ransom and H. Sontheimer, J. Neurophysiol. **85**, 790 (2001).
[8] A. Zholos, L. Baidan, A. Starodub, and J. Wood, Neuroscience **2**, 603 (1999).
[9] MP Mahaut-Smith, J. Physiol. (London) **484**, 15 (1995).
[10] V. Malev, L. Schagina, P. Gurnev, J. Takemoto, E. Nestorovich, and S. Bezrukov, Biophys. J. **82**, 1985 (2002).
[11] Z. Lu and R. MacKinnon, J. Gen. Physiol. **104**, 477 (1994).
[12] T. Rostovtseva, V. Aguilella, I. Vodyanoy, S. Bezrukov, and V.A. Parsegian, Biophys. J. **75**, 1783 (1998).
[13] B. Sakmann and G. Trube, J. Physiol. (London) **347**, 641 (1984).
[14] A. Lopatin and C. Nichols, Biophys. J. **71**, 682 (1996).
[15] A. Aleksandrov, B. Velimirovic, and D.E. Clapham, Biophys. J. **70**, 2680 (1996).
[16] P. Horowicz, P.W. Gage, and R.S. Eisenberg, J. Gen. Physiol. **51**, 193s (1968).
[17] B.C. Spalding, O. Senyk, J.G. Swift, and P. Horowicz, Am. J. Physiol. **241**, C68 (1981).
[18] B.C. Spalding, J.G. Swift, and P. Horowicz, J. Membr. Biol. **93**, 141 (1986).
[19] M.F. Schumaker and R. MacKinnon, Biophys. J. **58**, 975 (1990).
[20] D. Chen *et al.*, Biophys. J. **73**, 1337 (1997).
[21] R.S. Eisenberg, J. Membr. Biol. **171**, 1 (1999).
[22] D.G. Levitt, Biophys. J. **48**, 19 (1985).
[23] P.C. Jordan, R.J. Bacquet, J.A. McCammon, and P. Tran, Biophys. J. **55**, 1041 (1989).
[24] T. Allen, O.F. Andersen, and B. Roux, Proc. Natl. Acad. Sci. U.S.A. **101**, 117 (2004).
[25] T. Allen, T. Batu, S. Kuyucak, and S. Chung, Biophys. J. **84**, 2159 (2003).
[26] S. Bernèche and B. Roux, Biophys. J. **78**, 2900 (2000).
[27] A. Mamonov, R. Coalson, A. Nitzan, and M.G. Kurnikova, Biophys. J. **84**, 3646 (2003).
[28] R.S. Eisenberg, J. Membr. Biol. **115**, 1 (1990).
[29] G. Moy, B. Corry, S. Kuyucak, and S. Chung, Biophys. J. **78**, 2349 (2000).
[30] B. Corry, S. Kuyucak, and S. Chung, Biophys. J. **78**, 2364 (2000).
[31] P. Graf, A. Nitzan, M.G. Kurnikova, and R.D. Coalson, J. Phys. Chem. B **104**, 12 324 (2000).
[32] P. Graf, M.G. Kurnikova, R.D. Coalson, and A. Nitzan, J. Phys. Chem. B **108**, 2006 (2004).
[33] Z. Schuss, B. Nadler, and R.S. Eisenberg, Phys. Rev. E **64**, 036116 (2001).
[34] B. Nadler, Z. Schuss, A. Singer, and R.S. Eisenberg, J. Phys.: Condens. Matter **16**, S2153 (2004).
[35] B. Nadler, U. Hollerbach, and R.S. Eisenberg, Phys. Rev. E **68**, 021905 (2003).
[36] D.G. Levitt, Curr. Top. Membr. Transp. **21**, 181 (1984).
[37] E. Jakobsson and S.W. Chiu, Biophys. J. **52**, 33 (1987).
[38] P. McGill and M.F. Schumaker, Biophys. J. **71**, 1723 (1996).
[39] J.N. Aqua and F. Cornu, J. Stat. Phys. **105**, 211 (2001).
[40] R.S. Eisenberg, M.M. Klosek, and Z. Schuss, J. Chem. Phys. **203**, 1767 (1995).
[41] J. Barthel *et al.*, *Physical Chemistry of Electrolyte Solutions: Modern Aspects* (Springer, New York, 1998).
[42] S. Durand-Vidal *et al.*, *Electrolytes at Interfaces* (Kluwer, Boston, 2000).
[43] B. Nadler, U. Hollerbach, and R.S. Eisenberg (unpublished).
[44] J.P. Simonin *et al.*, J. Phys. Chem. **100**, 7704 (1996).
[45] A. McBride, M. Kohonen, and P. Attard, J. Chem. Phys. **109**,

2423 (1998).
[46] J. Rosgen *et al.*, J. Phys. Chem. B **108**, 2048 (2004).
[47] R.S. Eisenberg, Biophys. Chem. **100**, 507 (2003).
[48] D. Gillespie *et al.*, J. Phys.: Condens. Matter **14**, 12 129 (2002).
[49] W. Nonner *et al.*, Biophys. J. **79**, 1976 (2000).
[50] W. Nonner *et al.*, J. Phys. Chem. B **105**, 6427 (2001).
[51] A. Koumanov, U. Zachariae, H. Engelhardt, and A. Karshikoff, Eur. Biophys. J. **32**, 689 (2003).
[52] F. Stillinger, J. Chem. Phys. **35**, 1584 (1961).